Spring 5-2-2011

A Practical Model for a Dense- Bed Countercurrent FCC Regenerator

Yongmin Zhang
China University of Petroleum, China

Chunxi Lu
Chinese University of Petroleum (Beijing), lcxing@cup.edu.cn

A PRACTICAL MODEL FOR A DENSE-BED COUNTERCURRENT FCC REGENERATOR

Yongmin Zhang, Chunxi Lu
State Key Laboratory of Heavy Oil Processing, China University of Petroleum, Beijing, 102249, P. R. China

Abstract
In this study, a new practical countercurrent regenerator model for in-situ FCC operation optimization was proposed. A three-zone-and-two-phase gas model and a new two-CSTR-with-interchange model were used to give better descriptions on the gas and solids flow patterns, addressing the region-dependent mass transfer rates and the freeboard effect on catalyst regeneration. The model coupled mass and heat balances, hydrodynamics and reaction kinetics. The modeled results are in reasonable agreement with the commercial data from an industrial FCC regenerator under both partial and full CO combustion modes.

INTRODUCTION

A regenerator is an indispensable part of a FCC unit, acting as a fluidized-bed reactor to burn the coke deposited in the spent catalyst and recover its cracking activity. An ideal FCC regenerator requires very low levels of carbon content in regenerated catalyst (CCR) (0.05~0.1 wt%) with minimized air consumption and maximized coke burning intensity (CBI) (usually defined as weight of coke burned for a given catalyst inventory and a given period). A practical regenerator model based on sound understanding of its intrinsic hydrodynamics, mixing and reaction kinetics is undoubtedly valuable to optimization of its design and operation.

There have been several published studies on modeling dense-bed FCC regenerators (1-7). However, they all failed to describe the gas and solids flow patterns properly in the three zones (grid zone, dense-bed zone and freeboard zone) of a regenerator simultaneously, resulting in modeled results divergent largely from experimental facts and low reliability and predictability. Some of them (1-5) used the simple Orcutt fluidized-bed model (8) to model gas flow in the dense bed, which falsely modeled the reactant gas concentration in the emulsion phase to be a constant level. Otherwise, only Lu (5) and De Lasa et al. (7) considered the large amount of particles entrained in the freeboard and the associated reactions. However, Lu (5) improperly modeled the solid flow in the freeboard with a multiple-CSTR-in-series model, which over-predicted the freeboard reaction. The freeboard model of De Lasa et al. (7) was a particle-trajectory based model, which was too complex to use in engineering practice.

The goal of this study is to establish a modified model for a countercurrent regenerator. This model has a modified hydrodynamic model that provides better descriptions for gas and solid flows in both dense bed and freeboard. Otherwise, its structure still remains simple enough to be a practical engineering tool.

MODEL SCHEME

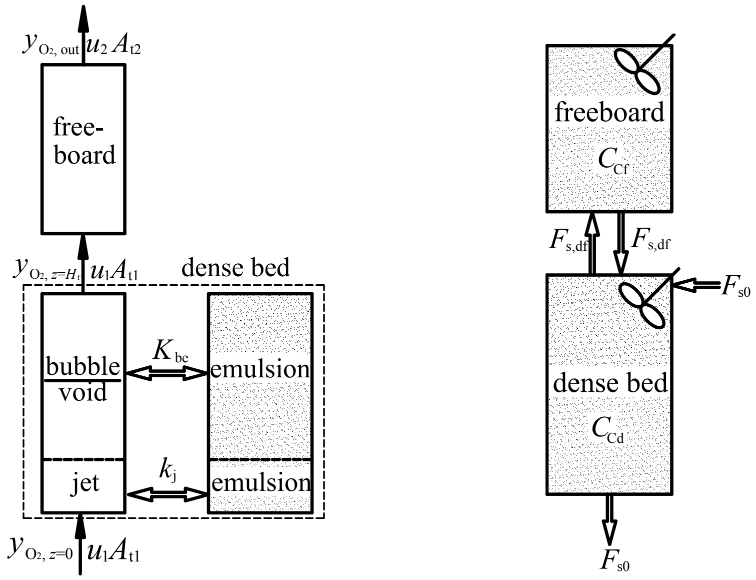

(a) (b)

Fig. 1 Gas and solid flow patterns in the countercurrent FCC regenerator model: (a) gas flow pattern; (b) solid flow pattern

A countercurrent regenerator is usually the preferred choice in a FCC unit for its better performance, where catalysts are usually injected to the top of its dense bed by a specially designed catalyst distributor, and withdrawn through the bed bottom. Figure 1 illustrates the hydrodynamic models describing the gas and solid flow patterns in this study. For the gas flow in the dense bed, a simple two-phase bubbling-bed model proposed by Chavarie and Grace (9) is used. This is a two-phase model with a "stagnant" emulsion phase, i.e. gas in the emulsion phase coming only from mass transfer from the bubble phase and without axial dispersion. Different from the Orcutt model (8), there is an axial gradient for the reactant gas concentration in the emulsion phase in agreement with experimental facts. Axially, two zones were partitioned in the dense bed to address the different gas transfer rates between emulsion and voids in the bubbling zone and jets in the jet zone. In the freeboard, the gas phase becomes a continuous phase, where interphase mass transfer becomes less important than in the dense bed. Gas flows in the jets, voids and freeboard were all modeled as plug flow without back-mixing. For an irreversible first order reaction $A \rightarrow B$ with negligible volume change, mole balances on A in the bubble phase and emulsion phase yield, respectively,

$$u_0 \frac{dC_{A\mathrm{b}}}{dz} + k_{\mathrm{be}}\alpha_{\mathrm{b}}\delta_{\mathrm{b}}\left(C_{A\mathrm{b}} - C_{A\mathrm{e}}\right) + k_{\mathrm{r}} f_{\mathrm{sb}} C_{A\mathrm{b}} = 0\,, \tag{1}$$

$$k_{\mathrm{be}}\alpha_{\mathrm{b}}\delta_{\mathrm{b}}\left(C_{A\mathrm{e}} - C_{A\mathrm{b}}\right) = k_{\mathrm{r}} f_{\mathrm{se}} C_{A\mathrm{e}}\,. \tag{2}$$

For the solids flow, a two-CSTR-with-interchange model shown in Fig. 1(b) was adopted. A distinct difference in this model lies in its different manipulation on solid flow in the freeboard. In a typical fluidized bed, particles in the freeboard come mainly from bubble eruptions on the bed surface. Particle concentration and upward flux decrease exponentially with increasing distance from the bed surface. Only a negligibly small fraction of particle leaves from the freeboard top and is captured by cyclones. This demonstrates that most solid inventory in freeboard exists within a small-height zone near the bed surface, i.e. the so called splash zone. In this zone, violent mixing due to strong gas flow turbulence and large solids exchange rate between the dense bed and the freeboard can be expected. Therefore, solids flow in freeboard was modeled as a separate CSTR reactor with solid exchange with the dense bed in this model. Physically, freeboard in this model is to provide particles with additional time to burn coke with negligible interphase mass transfer resistance.

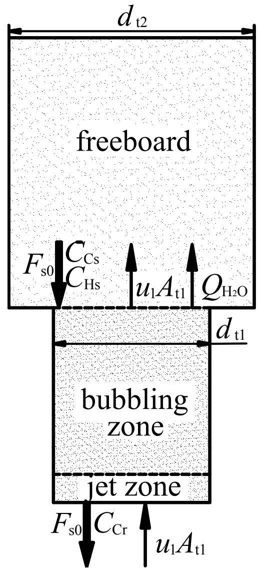

Fig. 2 Geometry model for an FCC regenerator with an expanded freeboard

Other simplifications are assumed to facilitate the modeling. First, the hydrogen content of the coke is assumed to combust instantly near the bed surface due to the much higher combustion rate of hydrogen (usually an order faster than carbon combustion) (10). Second, the structure of the FCC regenerator is simplified as showed in Fig. 2. The bottom bed section is always assumed to have the same height as the dense bed, H_f, whereas the expanded top section is assumed to be a cylinder of diameter d_{t2} and height H_t-H_f.

MODEL SETUP

Kinetic Model

Due to the simplification for hydrogen combustion, only carbon combustion needs to be considered in this model. Carbon combustion can be described by

$$\mathrm{C}+\frac{2\beta+1}{2(\beta+1)}\mathrm{O_2}\rightarrow\left(\frac{\beta}{\beta+1}\right)\mathrm{CO_2}+\left(\frac{1}{\beta+1}\right)\mathrm{CO} \quad (3)$$

where β is the ratio of CO2 to CO released. β is affected by many factors including catalyst type, feedstock, temperature, contents of oxygen and CO promoter etc. In this model, β is simply determined as the ratio of CO2 and CO concentrations in the flue gas of the modeled regenerator. This also simplifies the complex homogeneous and heterogeneous CO combustion procedures in actual conditions. The carbon combustion rate is estimated by (11)

$$k_{\mathrm{C}} = 2.967\exp\left(-\frac{1.422\times10^{5}}{RT}\right). \tag{4}$$

Hydrodynamics Model

Two important parameters in the grid zone, jet length and jet diameter, are determined by Lu's correlations (5).

$$L_{\mathrm{j}} = 141.85 d_{\mathrm{or}} \left(\frac{\rho_{\mathrm{p}} d_{\mathrm{p}}}{\rho_{\mathrm{g}} d_{\mathrm{or}}}\right)^{0.273} \left(\frac{\rho_{\mathrm{g}} u_{\mathrm{or}} d_{\mathrm{or}}}{\mu_{\mathrm{g}}}\right)^{-0.654} \left(\frac{u_{\mathrm{or}}^{2}}{g d_{\mathrm{or}}}\right)^{0.408}, \tag{5}$$

$$D_{\mathrm{j}} = 0.388 d_{\mathrm{or}} \left(\frac{u_{\mathrm{or}}^{2}}{g d_{\mathrm{or}}}\right)^{0.332}. \tag{6}$$

The average bed density is also determined based on the measured industrial data as expressed by Eqs. (7) and (8). The derivative in Eq. (8) is derived from a correlation of Cai et al. (12)

$$\rho_{\mathrm{B}} = \rho_{\mathrm{B,exp}} + \frac{\partial \rho_{\mathrm{B}}}{\partial u_{1}}\left(u_{1} - u_{1\mathrm{e}}\right) \tag{7}$$

$$\frac{\partial \rho_{\mathrm{B}}}{\partial u_{1}} = \frac{\partial\left[\rho_{\mathrm{p}}\left(1-\varepsilon\right)\right]}{\partial u_{1}} = -\frac{3n\left(\rho_{\mathrm{p}} - \rho_{\mathrm{B,exp}}\right)}{u_{1}} \tag{8}$$

The dense bed height and the axial particle concentration profile are determined based on Zhang et al. (13), which considered the solid mass balance of the whole regenerator. The solid fraction in the freeboard is expressed as

$$f_{\mathrm{s}} = f_{\mathrm{s}}^{*} + \left(f_{\mathrm{s}}^{0} - f_{\mathrm{s}}^{*}\right)\exp\left(-a z_{\mathrm{f}}\right), \tag{9}$$

where f_s^* is the saturated solids fraction, determined by measured cyclone inlet concentration in this study, f_s^0 is the initial solid fraction at the bed surface and determined by

$$f_{\mathrm{s}}^{0} = \frac{0.3\left(u_{1} - u_{\mathrm{mf}}\right)\left(1-\varepsilon_{\mathrm{mf}}\right)A_{\mathrm{t1}}}{A_{\mathrm{t2}} u_{\mathrm{b}}}. \tag{10}$$

Here, u_b is void rise velocity determined by the ratio of superficial gas velocity and bubble fraction in the dense bed, i.e. u_1/ $_b$; the exponent coefficient . is determined by 0.7/u_2 according to Zhang et al. (13). Based on mass balance in the regenerator,

$$\rho_{\mathrm{B}} H_{\mathrm{f}} A_{\mathrm{t1}} + \rho_{\mathrm{p}} A_{\mathrm{t2}} \int_{0}^{H_{\mathrm{t}}-H_{\mathrm{f}}} f_{\mathrm{s}} dz_{\mathrm{f}} = M_{\mathrm{s}}, \tag{11}$$

the dense bed height H_f can be determined.

Gas transfer coefficient between jet and emulsion is estimated by Lu's correlation (7),

$$k_{\mathrm{j}} = 0.48\left(\frac{d_{\mathrm{or}} u_{\mathrm{or}} \rho_{\mathrm{g,j}}}{L_{\mathrm{j}}}\right)\left(\frac{u_{\mathrm{or}}^{2}}{g L_{\mathrm{j}}}\right)^{-0.504}\left(\frac{L_{\mathrm{j}}}{d_{\mathrm{or}}}\right)^{0.905}\left(\frac{d_{\mathrm{or}} u_{\mathrm{or}} \rho_{\mathrm{g,j}}}{u_{\mathrm{g,j}}}\right)^{0.068}. \tag{12}$$

Bubble-emulsion gas transfer coefficient is estimated by De Groot' s correlation (14),

$$K_{\mathrm{be}} = k_{\mathrm{be}} a_{\mathrm{b}} = \frac{u_1}{0.67 H_{\mathrm{f}}^{0.5} d_{\mathrm{t1}}^{0.25}}, \tag{13}$$

which omits the need to know the average bubble size, a very difficult parameter to estimate in large-scale industrial fluidized beds.

Mass and Heat Balances

To determine the profiles of gas components, carbon content in the catalyst and temperature in the regenerator, the oxygen balance, carbon balance and heat balance are needed in the model. Due to page limit here, these procedures are only briefly introduced in the following text.

During the regeneration process, changes of gas compositions, carbon content and temperature are interrelated. Their values need to be solved together. Oxygen balance in the dense bed is based on Chavarie and Grace (14) with consideration of different mass transfer rates in the grid and bubbling zones. In the freeboard, interphase mass transfer is neglected, with reaction kinetics as the controlling factor. With oxygen concentration, concentrations of CO_2 and CO are readily known according to the reaction formula shown in Eq. (3). The profile of carbon content is determined according to the solids flow model and the consumption of oxygen. In this model, the carbon contents in the dense bed and freeboard are constant due to the completely mixed assumption. With higher mass transfer rate, the carbon content in the freeboard is a little lower than in the dense bed. The heat balance needs to consider the heat input from combustion of carbon and hydrogen, heat to heat up the influent air and spent catalyst, heat loss to atmosphere from the outside shell, and heat removed from catalyst coolers.

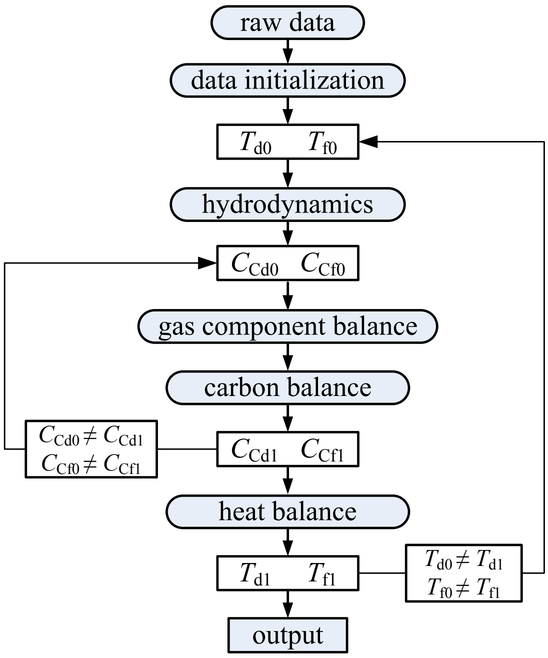

Fig. 3 Flow chart of model program

Solving Algorithm

This model is programmed in Matlab language using a modularized scheme and solved by an iterative method as shown in Fig. 3. There are seven modules and two iteration loops. To establish a model for optimizing the operation of a specified FCC regenerator, a calibration procedure is required to determine key unit-dependent parameters based on existing industrial data. Then, basic operating data can be changed to see their effects on the performance of the regenerator and to determine optimized operating parameters.

MODEL VALIDATIONS AND DISCUSSION

Table 1 A comparison of the modeled results and industrial data

Items		**Partial mode**		**Full mode**	
Catalyst inventory, ton		185		160	
Superficial gas velocity in the dense bed, m/s		0.85		0.93	
Superficial gas velocity in the freeboard, m/s		0.48		0.52	
Items for comparison		**Model**	**Exp.**	**Model**	**Exp.**
Bed height of dense bed, m		7.91		8.05	
Bed density, kg/m^3		278	276	221	220
Freeboard density, kg/m^3		10.9	12	14.9	14
Dense bed temperature, °C		660	662	689	690
Freeboard temperature, °C		669	670	696	699
Carbon content of the spent catalyst, (wt) %		1.49		1.74	
Carbon content of the regenerated catalyst, (wt) %		0.18	0.15	0.038	0.05
CBI, kg/(h.ton (cat.))		102.1	105.7	112.8	106.7
Components of flue gas (dry), v%	O_2	0.89	0.8	3.31	3.1
	CO	1.61	1.6	0.31	0.3
	CO_2	16.88	16.8	15.8	15.4

Industrial data from a FCC unit in Luoyang Petrochemical Corporation, Sinopec were used to compare with the modeled results. This FCC unit has a coaxial reactor-regenerator layout, processing 1.4 million tons of atmospheric residue per year. A single-stage countercurrent regenerator is used to regenerate the spent catalyst. The regenerator was first operated in the full CO combustion mode with a CO promoter. Later, in order to increase the processing capacity and decrease the main air flow rate, the regenerator was revamped to partial CO combustion mode with reduced air flow rate and without CO promoter. An advantage of this model is that only one fitting parameter, i.e. the interchanging solids flux between the dense bed and the freeboard, $F_{s,df}$, is used, which was determined based on the difference of temperature in the dense bed and freeboard. With a same $F_{s,df}$, both regeneration modes are modeled. The modeled results are compared with industrial data in Table 1. The main modeled hydrodynamic and performance results are in reasonable agreement with the industrial data, demonstrating the feasibility of this model.

With this model, the axial profiles of voidage, temperature, gas components and carbon content can be predicted, as shown in Fig. 4 for a typical partial CO combustion mode. It can be seen that most of the solids inventory in the freeboard is concentrated within a ~2 m high from the bed surface, where solids mixing is vigorous and a large solids exchange flux exists between the dense bed and freeboard. Therefore, there is only a small temperature increase in the freeboard, as seen in Fig. 4(b). Due to the different mass transfer rates, oxygen concentration decreases much sharply in the grid zone than in the bubbling zone. In the grid zone, the difference of oxygen concentration in the emulsion and dilute phases is much lower than in the bubbling zone. Due to higher mass transfer rate, carbon burns more efficiently in the freeboard, as indicated by the lower carbon content shown in Fig. 4 (d).

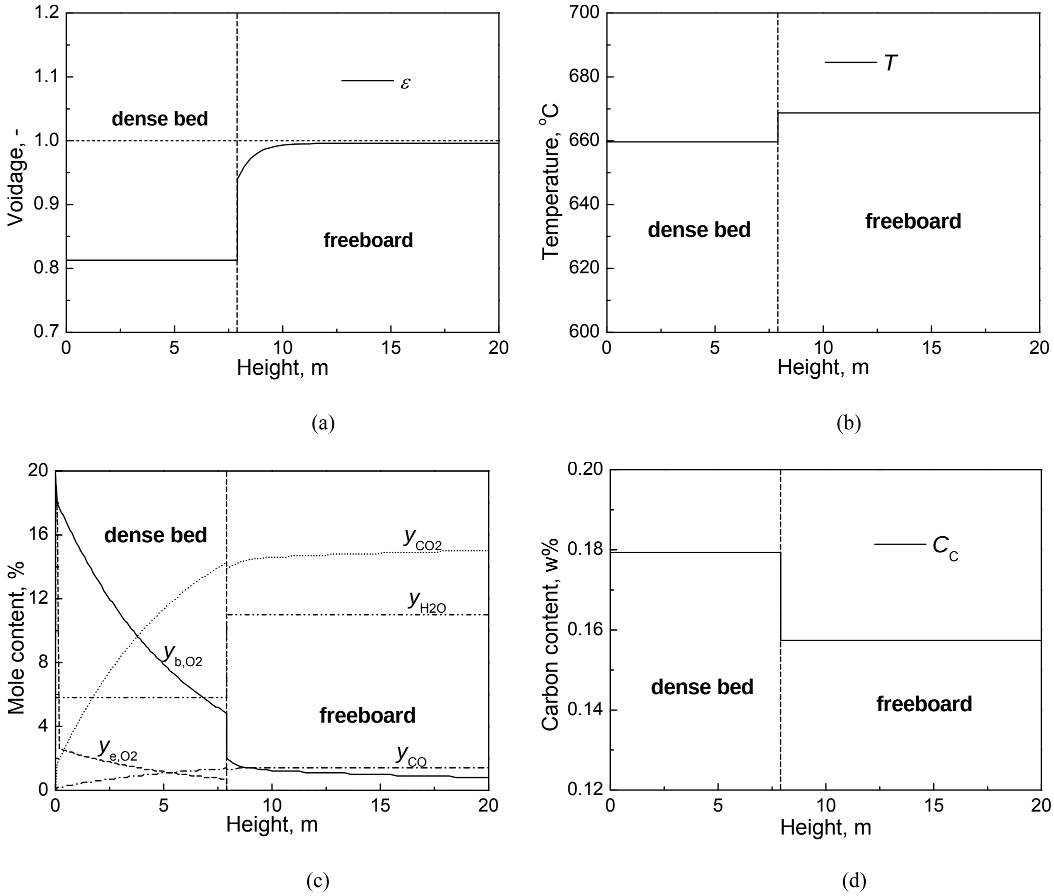

Fig. 4 Predicted profiles of (a) voidage, (b) temperature, (c) gas composition, and (d) carbon content under partial CO combustion mode

CONCLUSION

In this study, a modified countercurrent FCC regenerator model is proposed based on modified gas and solids flow patterns. The gas flow pattern in dense bed employs the "two-phase bubbling bed model" proposed by Chavarie and Grace (8), which can predict gas concentration profiles in better agreement with experimental facts. The modification in solids flow patterns focuses on the solids flow in freeboard, which was modeled as another CSTR exchanging solid with the dense bed. The model was applied to an industrial FCC regenerator operated under both full and partial CO combustion modes with agreeable modeled results obtainable with industrial data for both modes.

NOTATION

A_t bed area, m^2
C gas concentration, -
C_C carbon content, -
d diameter, m
d_t bed diameters, m
f_s solid volume fraction, -
$F_{s,df}$ interchange solid rate, $kg/m^2.s$
k_{be} bubble-emulsion mass transfer coefficient, m/s
K_{be} bubble-emulsion mass transfer coefficient, 1/s
k_j jet-emulsion mass transfer coefficient, $kg/m^2.s$
k_f reaction constant, 1/s
R gas law constant, kj/(kmol.K)
T temperature, K
H_f dense bed height, m
L_j jet length, m
M mass, kg
u superficial gas velocity, m/s
y concentration, -
z height, m
α coefficient, 1/m
α_b interphase area per volume of bubble, m^2/m^3
β CO_2/CO, -
δ_b bubble fraction, -
ε void fraction, -
ρ density, kg/m^3;

Subscripts

b bubble/bed
e emulsion
d dense bed
s solid
f freeboard
g gas
j jet
mf minimum fluidization
p particle
or orifice
0 initial
1(2) dense bed (freeboard)
* saturated

REFERENCES

1. Ford, F. D., Reinmen, R. C., Vasalos, I. A., and Fahrig, R. J., 1977. *Chem. Eng. Prog.* 73 (4): 92.
2. De Lasa, H. I., Errazu, A, Barreiro, E. And Solioz, S., 1981. *Can. J. Chem. Eng.* 59: 549-553.
3. Faltsi-Saravelou, O., Vasalos, I. A. And Dimogiorgas, G., 1991. *Comp. Chem. Eng.* 15: 647-656.
4. Filho, R. M., Batista, L. M. F. L. and Fusco, M., 1996. *Chem. Eng. Sci.* 51: 1807-1816.
5. Lu, C., 1996. Doctoral dissertation, *China University of Petroleum*, Beijing, China. (in Chinese)
6. Lee L. S., Yu, S. W., Cheng, C. T. and Pan, W. Y., 1989. *Chem. Eng. J.* 40: 71-82.
7. De Lasa, H. I. and Grace, J. R. 1979. *AIChE J.* 25: 984-991.
8. Orcutt, J. C., Davidson, J. F. and Pigford, R. L., 1962. *Chem. Eng. Prog. Symp. Ser.* 58: 1–15.
9. Chavarie, C. and Grace, J. R., 1975. *Ind. Eng. Chem. Fundam.* 14: 75-91.
10. Wang, G., Lin S., and Yang G., 1986. Ind. Eng. Chem. Proc. Des. Dev. 25: 626.
11. Dong, X. and Hao, X., 2006. *Petroleum Refinery Engineering*. 36 (6): 7-9. (in Chinese)
12. Cai, P., Jin, Y., Yu, Z. Q., and Wang, Z. W., 1990. *AIChE. J.* 36: 955-956.
13. Zhang Y. M., Lu C. X., Shi M. X., 2008. *Chem. Eng. Tech.* 31, 1735-1742.